



## Observation of the Crab Nebula with the MAGIC telescope

A. N. OTTE<sup>1,2</sup>, E. ALIU<sup>3</sup>, J. L. CONTRERAS<sup>4</sup>, M. GAUG<sup>5</sup>, M. LOPEZ<sup>4</sup>, P. MAJUMDAR<sup>1</sup>  
FOR THE MAGIC COLLABORATION

<sup>1</sup>*Max-Planck-Institut für Physik, D-80805 München, Germany*

<sup>2</sup>*Humboldt-Universität zu Berlin, D-12489 Berlin, Germany*

<sup>3</sup>*Institut de Física d'Altes Energies, Edifici Cn., E-08193 Bellaterra (Barcelona), Spain*

<sup>4</sup>*Universidad Complutense, E-28040 Madrid, Spain*

<sup>5</sup>*Università di Padova and INFN, I-35131 Padova, Italy*

otte@mppmu.mpg.de

**Abstract:** We report about very high energy (VHE)  $\gamma$ -ray observations of the Crab Nebula with the MAGIC telescope. The  $\gamma$ -ray flux from the nebula was measured between 60 GeV and 9 TeV. The energy spectrum can be described with a curved power law  $\frac{dF}{dE} = f_0 (E/300 \text{ GeV})^{(a+b \log_{10}(E/300 \text{ GeV}))}$  with a flux normalization  $f_0$  of  $(6.0 \pm 0.2_{\text{stat}}) \times 10^{-10} \text{ cm}^{-2} \text{ s}^{-1} \text{ TeV}^{-1}$ ,  $a = -2.31 \pm 0.06_{\text{stat}}$  and  $b = -0.26 \pm 0.07_{\text{stat}}$ . The position of the IC-peak is determined at  $(77 \pm 47) \text{ GeV}$ . Within the observation time and the experimental resolution of the telescope, the  $\gamma$ -ray emission is steady and pointlike. The emission's center of gravity coincides with the position of the pulsar. Pulsed  $\gamma$ -ray emission from the pulsar could not be detected. We constrain the cutoff energy of the spectrum to be less than  $\sim 30 \text{ GeV}$ , assuming that the differential energy spectrum has an exponential cutoff. For a super-exponential shape, the cutoff energy can be as high as  $\sim 60 \text{ GeV}$ .

## Introduction

The Crab Nebula is the remnant of a supernova explosion that occurred in 1054 A.D. at a distance of  $\sim 2 \text{ kpc}$ . It is one of the best studied non-thermal celestial objects in almost all wavelength bands of the electromagnetic spectrum from  $10^{-5} \text{ eV}$  (radio) to nearly  $10^{14} \text{ eV}$  ( $\gamma$ -rays). The radiation from radio to  $\gamma$ -rays ( $E \leq 1 \text{ GeV}$ ) is interpreted as synchrotron emission of relativistic electrons and positrons. At higher energies it is believed that inverse Compton scattering is the dominant generation process of  $\gamma$ -rays [8, 6, 12]. There is little doubt that the engine of the nebula is the pulsar PSR B0531+21 (hereafter Crab pulsar), which is also a strong source of  $\gamma$ -rays detected up to 10 GeV.

In very high energy (VHE)  $\gamma$ -ray astronomy the Crab nebula was first detected with large significance at TeV energies by the pioneering Whipple telescope [12]. Since then the Crab nebula was extensively studied by ground based experiments at

energies above a few hundred GeV. However, between 10 GeV and  $\sim 200 \text{ GeV}$ , observations are sparse.

Here we present highlights of an 16 hour observation of the Crab nebula and pulsar that was performed with the MAGIC telescope between October 2005 and December 2005. A more detailed discussion of the analysis and results presented here can be found in [3].

After a short description of the MAGIC telescope and the performed observations we present results from the analysis of the VHE- $\gamma$ -ray emission from the nebula and the search for pulsed emission from the pulsar. The paper is closed with some concluding remarks.

## The MAGIC telescope

The MAGIC (Major Atmospheric Gamma Imaging Cherenkov) telescope is located on the Canary Island La Palma (2200 m asl, 28.45°N, 17.54°W).

MAGIC is currently the largest single dish (17 m diameter) imaging atmospheric Cherenkov telescope (IACT). The faint Cherenkov light flashes produced in air showers are recorded by a camera comprising 577 photomultiplier tubes (PMTs). The central PMT is modified for optical pulsar studies [10].

The current configuration of the MAGIC camera has a trigger region of 2.0 degrees in diameter [5]. Presently, the trigger energy range spans from 50-60 GeV (at small zenith angles) up to tens of TeV.

## Analysis results of the Crab Nebula

### Source Morphology

The morphology of the  $\gamma$ -ray emission was studied by generating sky-maps in three different bins of energy. The center of gravity (CoG) of the  $\gamma$ -ray emission was derived from the sky-maps by fitting them with a 2D-Gaussian of the form

$$F_{\text{res}} + a \cdot \exp \left[ -\frac{(x - \bar{x})^2 + (y - \bar{y})^2}{2\sigma^2} \right], \quad (1)$$

where  $F_{\text{res}}$  is introduced to account for a possible constant offset of the background subtracted sky-map. The CoGs obtained from the fitted  $\bar{x}$  and  $\bar{y}$  are shown in Figure 1 superimposed on the composite image of optical, IR and X-ray observations of the Crab nebula. The three measured CoGs are compatible among each other and coincide with the position of the pulsar. Note that the systematic uncertainty of the position is about  $1'$ .

The extension of the  $\gamma$ -ray emission region is compatible with a point-like source. Upper limits on the source extension were calculated with a confidence level of 95%. The results for energies  $\sim 250$  GeV ( $< 2.4'$ ) and  $> 500$  GeV ( $< 1.6'$ ) are presented in Figure 1. In both cases the emission is constrained to originate from within the optical nebula.

### Energy spectrum

Figure 2 shows the differential flux measurements by MAGIC multiplied by the energy squared, i.e. the spectral energy density distribution. A parameterization of the spectrum with a power-law

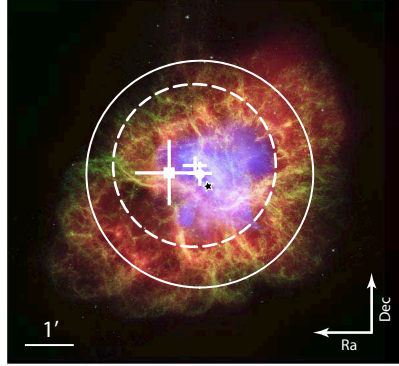


Figure 1: The crosses indicate the CoG of the VHE  $\gamma$ -ray emission at different energies (simple cross  $> 500$  GeV; dot  $\sim 250$  GeV; square  $\sim 160$  GeV), overlaid on an optical image from HST and an X-Ray image from Chandra. The position of the Crab pulsar is marked with a black star. The error bars indicate the statistical uncertainty in the position of the CoG. The upper limits on the 39% containment radius of the  $\gamma$ -ray emission region are indicated with circles (dashed  $> 500$  GeV; solid  $\sim 250$  GeV).

ansatz results in a  $\chi^2$  of 24 for 8 degrees of freedom. A better parameterization is obtained with a curved power-law ansatz.

$$\frac{dF}{dE} = f_0 (E/300 \text{ GeV})^{(a+b \log_{10}(E/300 \text{ GeV}))} \quad (2)$$

yielding a flux normalization  $f_0$  of  $(6.0 \pm 0.2_{\text{stat}}) \times 10^{-10} \text{ cm}^{-2} \text{ s}^{-1} \text{ TeV}^{-1}$ ,  $a = -2.31 \pm 0.06_{\text{stat}}$  and  $b = -0.26 \pm 0.07_{\text{stat}} \pm 0.2_{\text{syst}}$ . The  $\chi^2$  of the fit is 8 for 7 degrees of freedom.

For energies above 400 GeV the derived spectrum is in good agreement with measurements of other air Cherenkov telescopes. At energies  $< 400$  GeV, below the threshold of previous measurements by IACTs, we compare our results with integral flux measurements obtained by [7] and [11].

At lower energies one expects a continuous softening of the spectrum with increasing energy. However, this could not be demonstrated by earlier measurements. We derived spectral indices at  $\sim 150$  GeV,  $\sim 300$  GeV,  $\sim 1$  TeV and  $\sim 2.5$  TeV from the flux measurements as well as from the

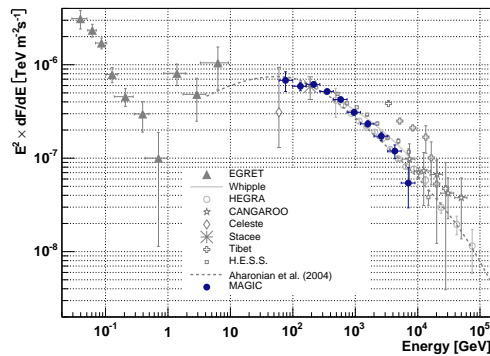


Figure 2: Spectral energy distribution of the  $\gamma$ -ray emission of Crab nebula. Below 10 GeV, measurements are by EGRET. In VHE  $\gamma$ -rays measurements are from ground-based experiments. The dashed line is a model prediction by [1].

aforementioned results of the curved power-law fit. The results, shown in Figure 3 together with several predictions, indicate a clear softening of the spectrum with increasing energy.

The predicted GeV  $\gamma$ -ray emission has a peak in the SED-representation (see Figure 2). If one assumes that the energy spectrum around the peak can be described with a curved power-law, we can determine the position of the peak from the curved power-law fit to be  $77 \pm 47_{\text{stat}}^{+107} -46_{\text{syst}}$  GeV.

Within statistical uncertainties, the flux of  $\gamma$ -rays was constant over the entire observation period. Tested timescales were between a few minutes up to months. The average integral flux above 200 GeV is  $(1.96 \pm 0.05_{\text{stat}}) \times 10^{-10} \text{ cm}^{-2} \text{ s}^{-1}$ .

## VHE- $\gamma$ -ray emission from the pulsar

Motivated by a possible pulsed  $\gamma$ -ray component at TeV energies [9], we searched for pulsed emission in five bins of reconstructed energy between 60 GeV and 9 TeV. However, a signature of periodicity was not found in any of the tested energy intervals. Derived 95% confidence level flux limits are shown in Figure 4.

We also performed a periodicity analysis optimized for a search of pulsed emission close to

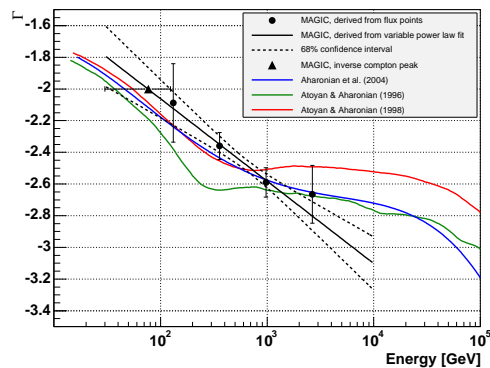


Figure 3: Spectral index derived from differential flux measurements (dots) and from the curved power-law fit (black solid line, the dashed line gives the  $1\sigma$  confidence interval); Predictions by [1] (blue curve), [4] (green curve) and [2] (red curve) are also shown.

the threshold of the experiment (analysis threshold 60 GeV). Figure 5 shows the resulting pulse phase profile together with EGRET data above 5 GeV and measurements in optical by MAGIC. An excess in VHE- $\gamma$ -rays is evident at the position of the inter-pulse in the same phase range where EGRET detected pulsed emission above 100 MeV (shaded region) and above 5 GeV. The MAGIC and EGRET  $> 5$  GeV pulse phase profile match with a probability of 87%. One calculates a significance of  $2.9\sigma$  of the excess if the phase regions where EGRET detected pulsed emission above 100 MeV (shaded regions) are defined as signal region and the remaining phase intervals as background region.

The observed excess is not sufficient to claim the detection of a pulsed signal, therefore, upper limits on the number of excess events were calculated with a confidence level of 95%. Using the limit on the number of pulsed excess events we constrained the cutoff energy of the pulsar spectrum to be less than 27 GeV, under the assumption that the break in the energy spectrum can be described with an exponential cutoff. In case the energy spectrum is attenuated super-exponentially, cutoff energies up to  $\sim 60$  GeV are allowed from our observations.

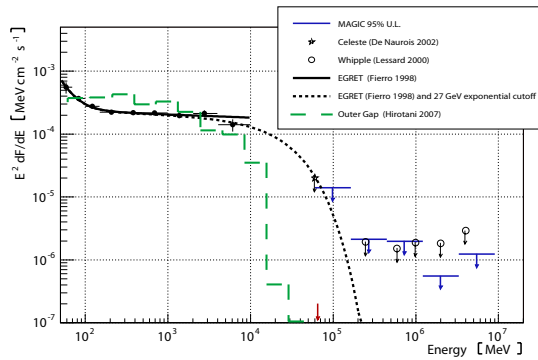


Figure 4: Upper limits on the pulsed gamma ray flux from the Crab pulsar; upper limits in differential bins of energy are given by the blue points. The upper limit on the cutoff energy of the pulsed emission is indicated by the dashed line.

## Concluding remarks

Here we reported on the currently most detailed study of the VHE  $\gamma$ -ray emission of the Crab nebula below 500 GeV. Most of the aforementioned studies were done in this energy region for the first time. Results from this study among others are a:

- measurement of the differential energy spectrum down to 60 GeV, which clearly deviates from a pure power-law behavior
- determination of the inverse Compton peak at  $77 \pm 47_{\text{stat}}^{+107}_{-46_{\text{syst}}}$  GeV
- point-like emission region with a CoG coinciding with the position of the pulsar
- constraint of the cutoff energy of the pulsar spectrum of  $\lesssim 27$  GeV, assuming an exponential cutoff

## Acknowledgements

We are grateful for discussions with Kouichi Hirotani. We also would like to thank the IAC for the excellent working conditions at the ORM in La Palma. The support of the German BMBF and MPG, the Italian INFN, the Spanish CICYT, ETH research grant TH 34/04 3, and the Polish MNiI grant 1P03D01028 are gratefully acknowledged.

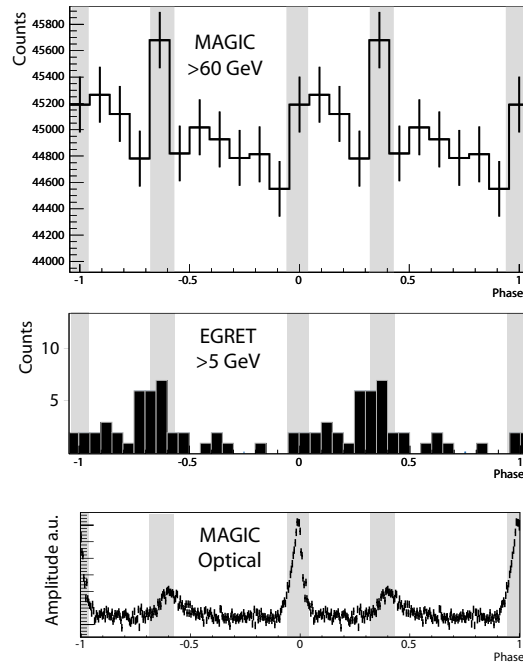


Figure 5: Pulse phase profiles of the Crab pulsar. Lower figure: optical observations by MAGIC; middle figure: observations by EGRET above 5 GeV; upper figure: pulse phase profile obtained by MAGIC. The shaded regions indicate the EGRET measured positions of the pulsed emission for  $\gamma$ -ray energies above 100 MeV.

## References

- [1] Aharonian et al. *ApJ*, 614:897, 2004.
- [2] F. A. Aharonian et al. In *Neutron Stars and Pulsars: Thirty Years after the Discovery*, page 439, 1998.
- [3] J. Albert et al. *astro-ph/0705.3244*, submitted to *ApJ*, 2007.
- [4] A. M. Atoyan et al. *MNRAS*, 278:525, 1996.
- [5] J. Cortina et al. In *ICRC*, page 359, 2005.
- [6] O. C. de Jager et al. *ApJ*, 396:161, 1992.
- [7] de Naurois et al. *ApJ*, 566:343, 2002.
- [8] R. J. Gould. *Phys. Rev. Lett.*, 15:577, 1965.
- [9] K. Hirotani. *ApJ*, 549:495, 2001.
- [10] F. Lucarelli et al. In *ICRC*, page 367, 2005.
- [11] Oser et al. *ApJ*, 547:949, 2001.
- [12] Weekes et al. *ApJ*, 342:379, 1989.